RMetS
Royal Meteorological Society

Contrasting impacts of spring thermal conditions over Tibetan Plateau on late-spring to early-summer precipitation in southeast China

Xiaodong Liu[1] and Yi Wang[1,2]*

[1] SKLLQG, Institute of Earth Environment, Chinese Academy of Sciences, Xi'an, China
[2] Department of Geography and School of Global Studies, University of Sussex, Falmer, Brighton, UK

*Correspondence to:
Yi Wang, Department of
Geography and School of Global
Studies, University of Sussex,
Falmer, Brighton BN1 9QJ, UK.
E-mail: yi.wang@sussex.ac.uk

Abstract

The thermal condition of the Tibetan Plateau (TP) is considered as an important factor impacting the Asian monsoon. However, how to determine the thermal condition and when and where the Asian monsoon is influenced are still open issues. Here the spring thermal condition of TP is determined using 600 hPa temperatures. For the past 30 years (1979–2008), we have determined three cold years (CY) and three warm years (WY) and conducted contrasting analyses of the subsequent precipitation and large-scale atmospheric dynamics over China. Our analyses indicate that the precipitation is more than normal in late spring (LS) and less than normal in early summer (ES) during WY in southeast China (SEC), while the opposite pattern is true during CY. Further analyses of 850 hPa circulation and tropospheric vertical motion show that the anomalous southerly wind and ascending motion are dominated in SEC during LS for WY and ES for CY, while the anomalous westerly wind and descending motion are dominated during ES for WY and LS for CY. The coherent dynamical structure impacts the monsoon moisture transport and large-scale atmospheric stability, and therefore is the fundamental cause of precipitation anomalies. Copyright © 2011 Royal Meteorological Society

Keywords: thermal conditions; Tibetan Plateau; Asian summer monsoon; atmospheric dynamics; atmospheric circulations; southeast China precipitation

1. Introduction

As the highest plateau in the world, the Tibetan Plateau (TP) has great impacts on the Asian summer monsoon (ASM) and climate changes due to its dynamical and thermal effects (Murakami, 1988; Yanai and Wu, 2006). As an elevated thermal source, TP directly heats the middle-upper tropospheric atmosphere, and hence largely affects the seasonal and interannual atmospheric circulations (Li and Yanai, 1996). Here we focus on the eastern branch of ASM, especially, that located near southeast China (SEC). The characteristics of Chinese subtropical rainfall are different from those of more convective rainfall over tropical South Asia. The seasonal rain bands over the mainland of China are considered to be related to the evolution of East ASM (EASM), and modulated by the thermal conditions of TP (Ding, 1992; Chang, 2004). Previous studies (Wu and Qian, 2003; Zhang *et al.*, 2004; Zhao *et al.*, 2007; Chow *et al.*, 2008; Zhou *et al.*, 2009) show that thermal anomalies of TP have impacts on the concurrent and/or lagged variations of EASM precipitation. For example, Hsu and Liu (2003) calculated the direct summer heating rates of TP, and found strong correlations between EASM and heating rates. Their results demonstrated that warm (cold) years of TP generally correspond to more (less) rainfall in the Yangtze River Basin in summer, and less (more) rainfall in northern and southern parts of China. Furthermore, winter and spring snow cover directly influences the surface albedo, soil moisture, and thermal conditions of TP, and therefore illustrates a significant correlation with EASM variations at interannual and decadal timescales (Wu and Qian, 2003; Zhang *et al.*, 2004; Zhao *et al.*, 2007; Ding *et al.*, 2009). Recent modeling studies (Qian *et al.*, 2003; Liu *et al.*, 2004; Zhou and Zou, 2010) also shed light on potential causing factors between TP snow covers and subsequent monsoon changes. More recently, soil moisture (Chow *et al.*, 2008) and vegetation (Wang *et al.*, 2009) were thought to affect thermal conditions of TP and therefore EASM.

Previous work mostly used surface and tropospheric temperatures, rates of sensible and adiabatic heating, and snow cover to represent thermal conditions of TP (Yanai and Wu, 2006; Wang *et al.*, 2008; Ding *et al.*, 2009). These studies showed the impact of TP thermal conditions on the seasonal and regional precipitation variations over East China. Because of the large population density, economy development and floods of recent decades, understanding the fundamental mechanisms of EASM variability is critical.

Different from previous work, we have focused on the spring–summer transition season of EASM. The
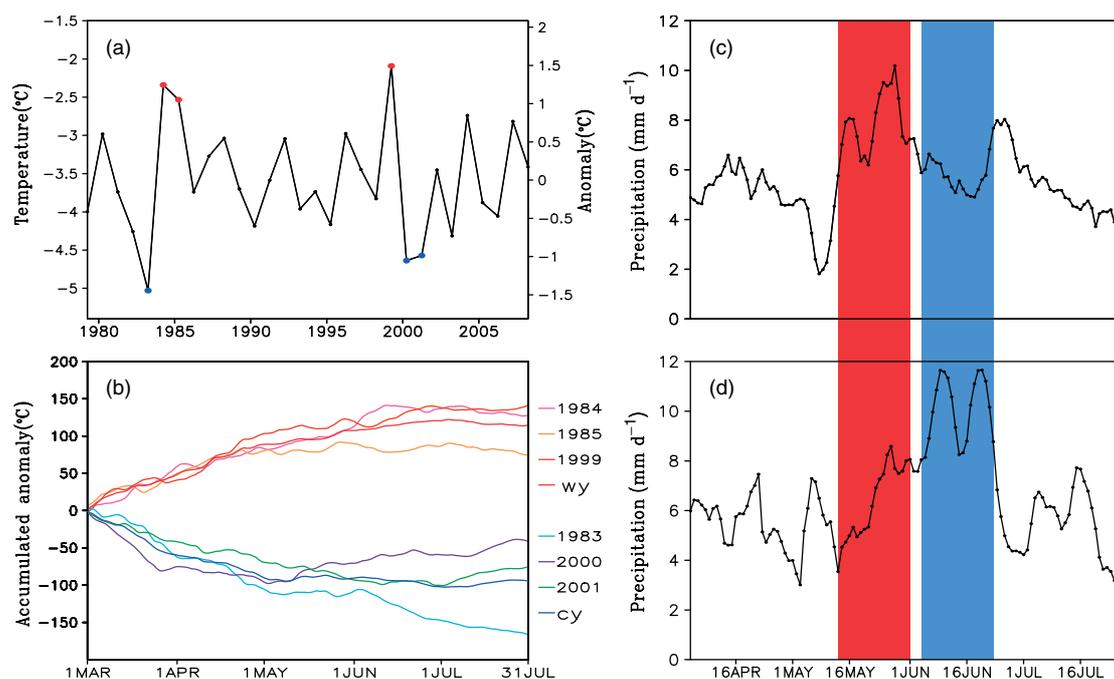
Figure 1. (a) Time series of yearly spring-mean 600 hPa temperature and anomaly averaged for the main part of Tibetan Plateau. (b) Accumulated temperature anomalies for the cold (1983, 2000, and 2001) and warm (1984, 1985, and 1999) years. (c) The composite of 7-day running average precipitation time series over SEC for WY. (d) Same as (c) but for CY. Notice that the mean accumulated temperature anomalies for CY and WY are denoted by the thicker blue and red lines in (b), respectively.

transition season corresponds to the northward advection of rain band in SEC, and therefore is a good proxy to predict the potential flood hazard therein. Specifically, we use data from NCEP-DOE reanalysis II (NCEP2) daily temperature and wind fields from 1979 to 2008 (Kanamitsu *et al.*, 2002) and NOAA Climate Prediction Center (CPC) daily gauge-based precipitation (resolution $0.5° \times 0.5°$) (Chen *et al.*, 2008). The NCEP2 data include 17 pressure levels and have a resolution of $2.5° \times 2.5°$. The data used here include meridional, zonal and vertical winds, and temperature. A few Chinese scientists (e.g., Wei and Li, 2003; Zhao and Fu, 2009) have used surface sounding data of TP to be compare with NCEP2. Although there are some differences between sounding and NCEP2, the spatial and temporal patterns of NCEP2 are still valid. Furthermore, we define the area of $80°–100°E$, $27.5°–37.5°N$ as the main part of TP, and SEC is defined as an area of $105.25°–122.25°E$, $22.25°–29.75°N$.

2. The selection of WY and CY of TP

How to define large-scale thermal conditions of TP is an active area of research. Because spring is the period that TP transits from a cold to a warm condition, surface sensible heat release has dominated thermal conditions of TP in spring, while the contribution of latent heat becomes important after the middle of May as the rainy season starts (Yanai and Wu, 2006). On the other hand, analyzing tropospheric temperatures at different pressure layers shows that 600 hPa is influenced most significantly by large-scale conditions of

TP. Because 600 hPa is closest to the surface of TP, temperature and circulation changes match those of the surface (Yin, 1986). Furthermore, 600 hPa is also the standard isobaric layer, in which the reversal of temperature gradient between TP and equator occurs the earliest from winter to summer. Li and Yanai (1996) discussed the significance of the reversal of temperature gradient between TP and its surroundings. Therefore, we define the thermal condition of TP as mean 600 hPa temperatures in the spring (1 March–15 May) from 1979 to 2008. Based on the temperature data from NCEP2, Figure 1(a) depicts 600 hPa temperatures and anomalies from the 30-year climatology. Spring mean temperatures are between $-1.6°C$ and $-5.6°C$, and anomalies are between $-2°C$ and $2°C$. Among the 30-year data, we find that 1984, 1985, and 1999 have the highest temperature [red spots in Figure 1(a), warm years (WY)]; while 1983, 2000, and 2001 have the lowest temperature [blue spots in Figure 1(a), cold years (CY)]. Our selection of WY and CY are different from Nan *et al.* (2009), who used average spring temperatures between 400 and 200 hPa.

We further analyze the daily accumulated temperature anomaly (departure from 30-year climatology) from March to July (Figure 1(b)). It is shown that the accumulative temperature anomaly is consistently positive for WY, while consistently negative for CY. The temperature anomaly is zero around 1st March, and starts to increase for WY and to decline for CY. By July, the maximum and minimum accumulated temperature anomaly years are 1999 (WY) and 1983
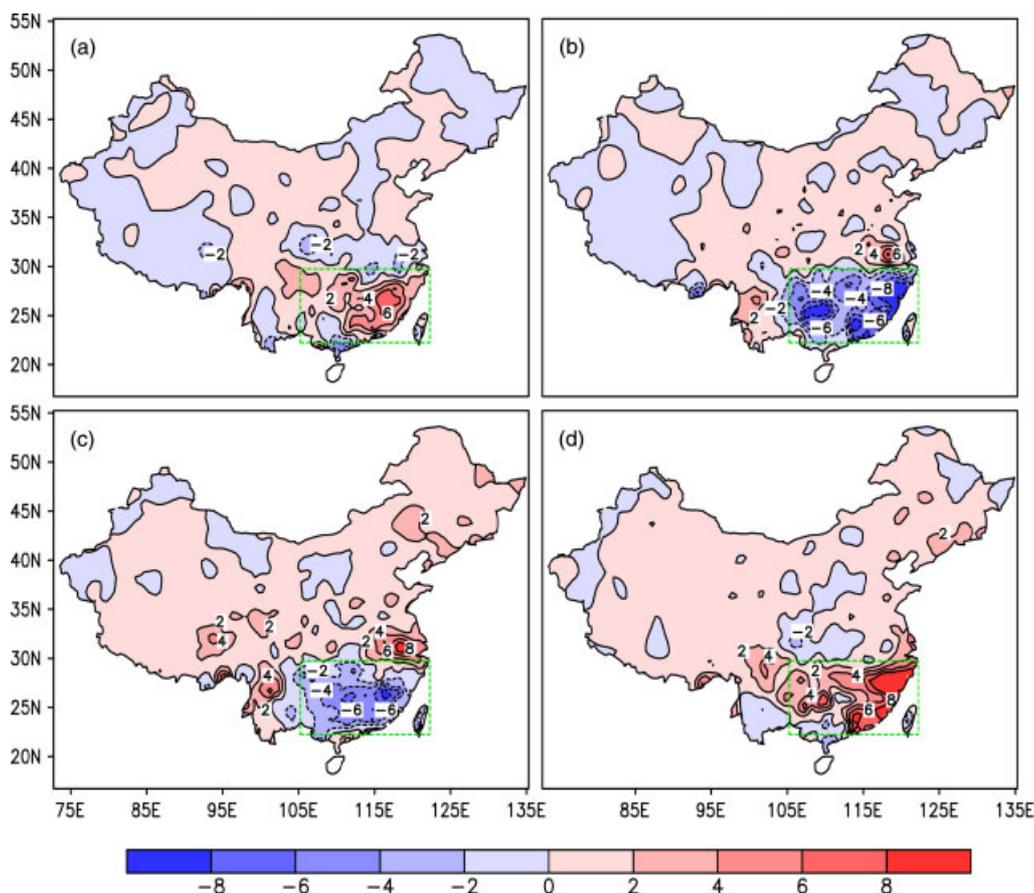
Figure 2. Contrasting changes of precipitation (mm/day) over China for LS and ES between WY and CY. (a) The precipitation difference between WY and CY (WY−CY) for LS. (b) Same as (a) but for ES. (c) The precipitation difference between ES and LS (ES-LS) for WY. (d) Same as (c) but for CY. Green boxes indicate SEC.

(CY), respectively. It is also noticeable that temperature anomaly trends for WY and CY slow down in June and further stabilize in July.

3. The spring–summer rainfall composite of southeast China

The rainy season in China generally begins with the onset of the summer monsoon and ends with its withdrawal (Zhou *et al.*, 2009). When the summer monsoon advances northward, the monsoon rain belt correspondingly moves from low latitudes to mid-high latitudes. In May and June, the major rain belt generally occurs south of 30 °N, thus causing the pre-summer major rainy season in SEC. Later the major rain belt rapidly shifts to the valley of Yangtze River, starting the so-called Meiyu (plum rains) season (mid-June to mid-July). There are strong contrasts between WY and CY with respect to the area-averaged precipitation anomaly in SEC (Figure 1(c) and (d)). A 7-day running average rainfall (mm/day) over SEC (denoted in Figure 2 as the green box) is composited for WY and CY from April to July (Figure 1(c) and (d)). In particular, during WY (Figure 1(c)), the late-spring (LS, 13 May–1 June) rainfall is the largest (red shade), while the early-summer (ES, 4 June–23 June)

rainfall is contrastingly less than that of LS (blue shade). On the other hand, during CY (Figure 1(d)), ES rainfall is the largest (blue shade), while LS rainfall is less than that of ES (red shade). Overall, strong contrasts have been found both between ES and LS for the same thermal condition of TP and between WY and CY for the same period of the year.

To illustrate the spatial pattern of rainfall anomalies during the spring–summer transition, we have composited the anomaly precipitation for WY and CY (figure not shown). It was found that during WY (CY), the subsequent rainfall anomaly during LS in SEC exhibits a large positive (negative) center, while the opposite is true for the rainfall anomaly during ES in SEC. We further composite the rainfall different between WY and CY (Figure 2, WY−CY), and find that (1) the largest precipitation difference between WY and CY occurs in SEC for both LS and ES; (2) during WY, SEC has more precipitation in LS than ES (Figure 2(a) and (b)); and (3) during CY, SEC has less precipitation in LS than ES (Figure 2(c) and (d)). Our analysis demonstrates that during the transition from spring to summer, there are significant rainfall contrasts between WY and CY, and also between LS and ES in SEC. It should also be noticeable that the remaining part of China does not exhibit such a strong
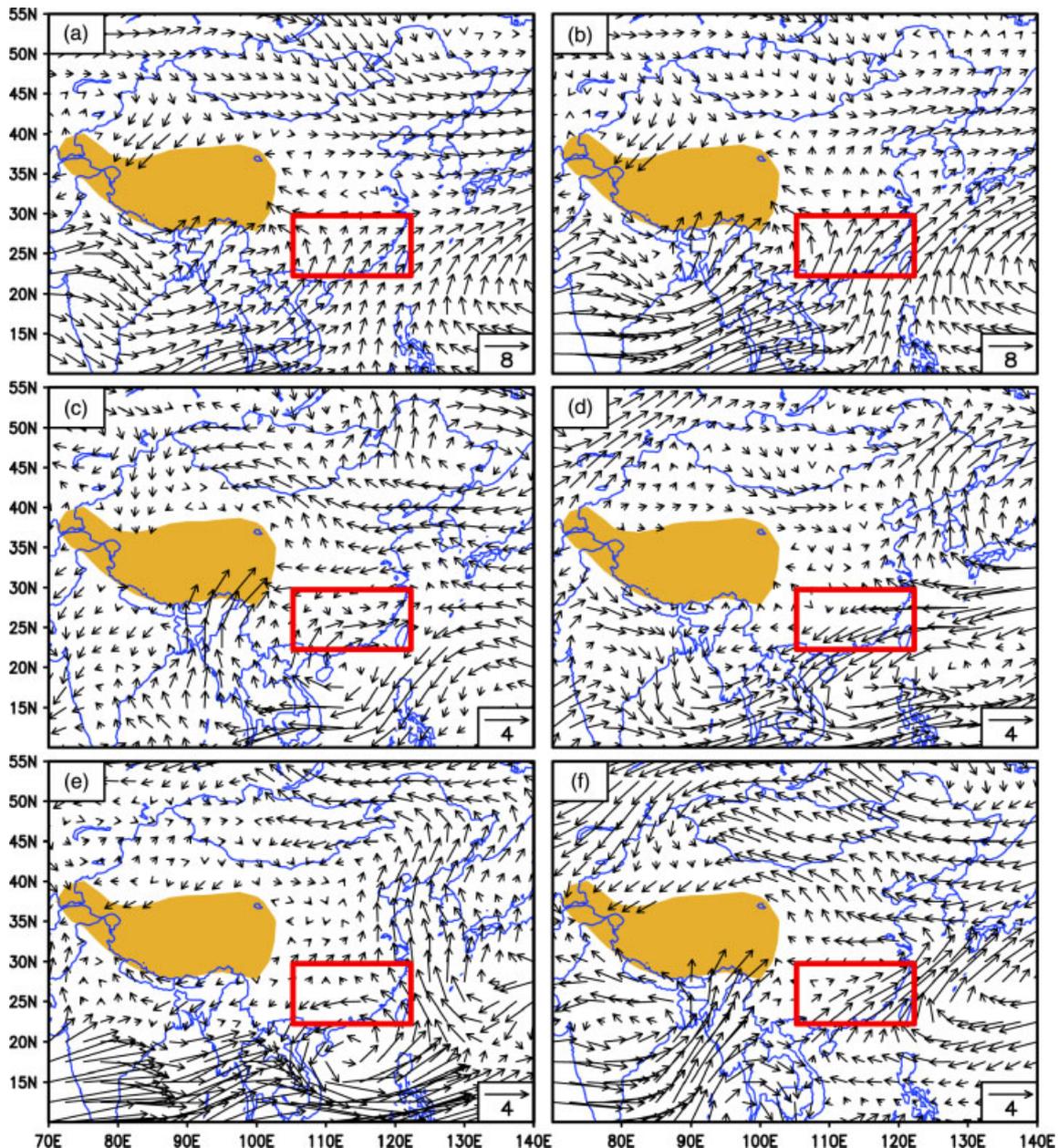
Figure 3. (a) The 850 hPa climatological wind field over East Asia for LS. (b) Same as (a) but for ES. (c) The difference of 850 hPa wind fields between WY and CY (WY−CY) for LS. (d) Same as (c) but for ES. (e) The difference of 850 hPa wind fields between ES and LS (ES−LS) for WY. (f) Same as (e) but for CY. Scales (m s^{-1}) are shown at lower-right corners for each panel. Red boxes indicate SEC and yellow shading areas represent the TP.

contrast in rainfall for WY and CY and for LS and ES (Figure 2).

4. The dynamics of WY and CY of TP

To detect the causing factors of rainfall contrasts above, we focused on the analysis of the 850 hPa circulations and vertical motions of the whole troposphere. The 850 hPa circulation determines the lower layer moisture transport, and hence affects the intensity and quantity of rainfall. The vertical motion of the whole troposphere could depict the large-scale atmospheric stability. During the LS to ES transition, India and southern Asia are dominated by northwesterly,

and the Bay of Bengal is dominated by westerly (Figure 3(a)). The southwesterly and southerly from the Chinese South Sea already reach SEC and the south of Yangtze River. While during the ES, Indian and southern Asia is dominated by westerly, and the Bay of Bengal is dominated by southwesterly. The southerlies are much stronger over SEC than those during the LS, and expanded to north of Yangtze River (Figure 3(b)). Based on the different circulation pattern between WY and CY (Figure 3, WY−CY), we find that the southerly in southern TP and SEC is stronger in LS (Figure 3(c)) and weaker in ES (Figure 3(d)). This is caused by the establishment of the thermal lower pressure system over TP (figure not shown), and the downstream
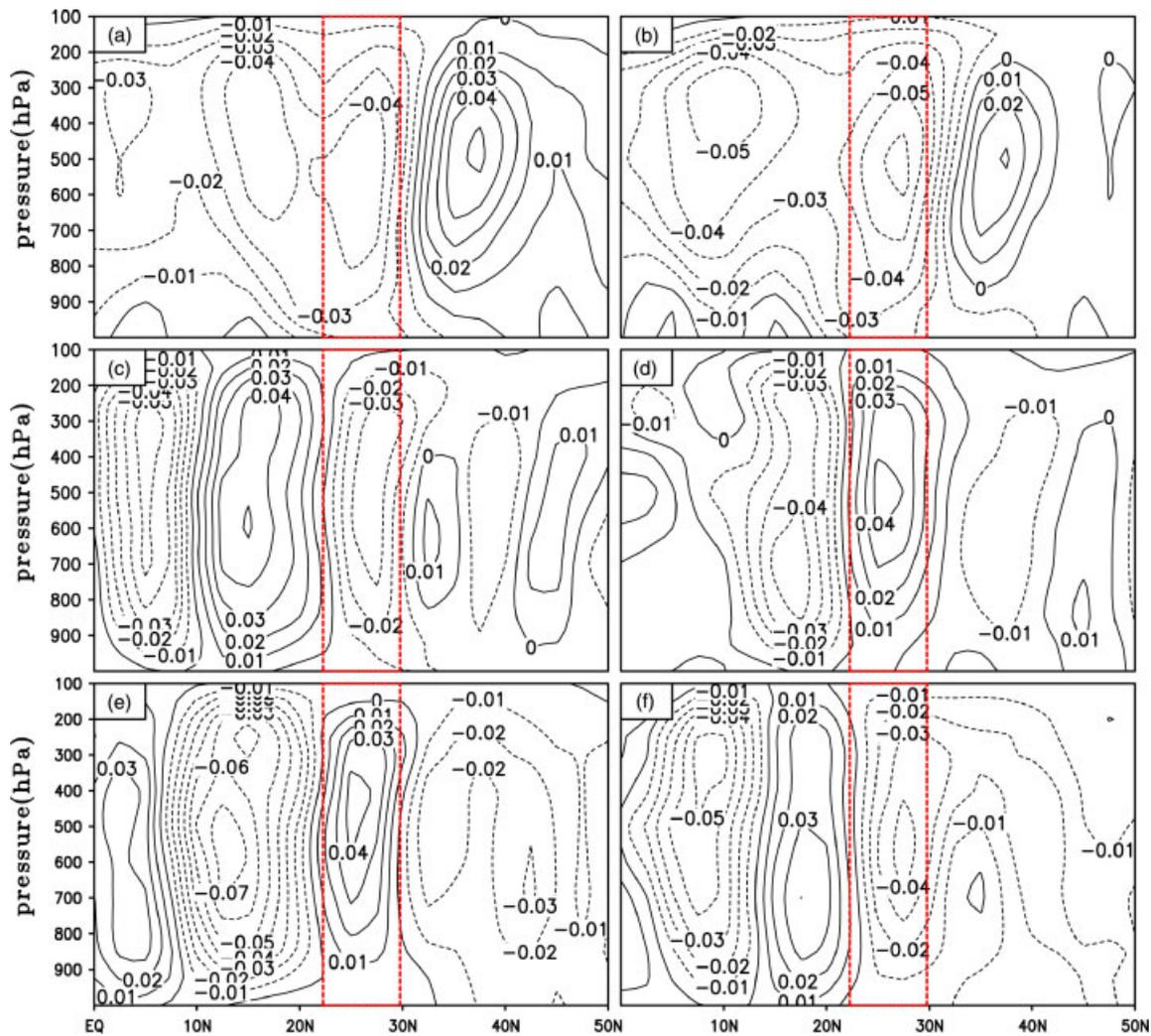
Figure 4. Latitude-height sections of climatology and contrasting changes of vertical p-velocity (ω, positive downward, Pa/s) averaged for the longitudinal band in the SEC (105.25°–122.25 °E). (a) The climatological ω for LS. (b) Same as (a) but for ES. (c) The ω difference between WY and CY (WY–CY) for LS. (d) Same as (c) but for ES. (e) The ω difference between ES and LS (ES–LS) for WY. (f) Same as (e) but for CY. Red boxes indicate SEC.

development of wavetrain perturbation, which make the western Pacific subtropical high develop earlier (later) in WY (CY). Corresponding to the subtropical high, the southerly anomaly generally appears in LS (ES) during WY (CY). Furthermore, during the WY, the southerly in SEC progresses slower from LS to ES (Figire 3(e)), while during the CY, it progresses faster (Figure 3(f)). This kind of circulation patterns has also shown clearly in the 850 hPa wind anomaly plot for WY and CY (figure not shown).

In the meantime, we estimate the mean vertical motion for SEC (averaging over the longitudinal band of 105.25°–122.25 °E). Based on the climatology of vertical motion, we note that during LS (Figure 4(a)), the tropical and subtropical zones (south of 30 °N) are dominated by ascending (negative ω), while north of 30 °N is dominated by descending (positive ω). During ES (Figure 4(b)), previous ascending motion zones are enhanced and expand toward the north. Corresponding to 850 hPa wind patterns, the vertical motion shows coherent patterns. For example, compared to CY, LS has stronger ascending motion in WY (Figure 4(c),

negative values in red box), while this strong upward motion becomes weaker late in ES (Figure 4(d)). Compared to WY, ES has a stronger ascending motion in CY (Figure 4(f)), while this strong upward motion becomes weaker early in LS (Figure 4(e)). Therefore, we can see the strong coherence between large-scale moisture transport and atmospheric stability (upward motion) in SEC. We suggest that this strong coherence is the primary causing factor leading to the precipitation anomaly in SEC. In addition, there is a meridional overturning circulation between the subtropical and tropical zones (Figure 4(c)–(f)); this phenomena and its effect on precipitation anomaly are an interesting subject of future research.

5. Summary and discussion

Here we used the 1979–2008 NCEP2 to derive the spring thermal condition in TP and its relationship with the subsequent EASM, and corresponding large-scale dynamics during the spring–summer transition.

Our analyses indicate significant correlations and contrasts in SEC rainfall both between WY and CY and between LS and ES. Our analyses also show strong coherence between large-scale moisture transport, tropospheric vertical motion, and rainfall in SEC. For example, when warm spring conditions dominate over TP (WY), the East Asian subtropical high develops earlier than normal; hence, the southerly in SEC is intensified during LS, as well as is a corresponding tropospheric ascending motion. The combination of moisture transport and vertical motion causes more precipitation in LS than in ES.

How to characterize the thermal condition of TP is a long-standing challenge. Although there were many studies to try to determine the thermal conditions using snow cover, surface and tropospheric temperature, and rates of sensible and adiabatic heating, there is no agreement. Here we introduce the 600 hPa temperature as a simple index to represent the thermal condition of TP. The 600 hPa temperature has (1) a strong correlation with large-scale surface sensible heating, (2) remarkable interannual variation, (3) good persistence, and (4) easy calculation, and therefore may be a practical tool for future seasonal and regional weather prediction of spring–summer precipitation in SEC.

Our conclusion is focused on the interannual variation of precipitation. There is a critical need to evaluate our conclusion over longer timescales (e.g., decadal). Observational studies show that TP snow cover has increased continuously since 1970s (Zhang *et al.*, 2004; Ding *et al.*, 2009), which may have reduced significantly the surface heating of TP and weakened the EASM circulation (Duan and Wu, 2008; Ding *et al.*, 2009). Therefore, whether the dry trend of SEC is caused by the weakened spring thermal condition of TP during recent decades needs to be investigated.

Finally, we want to point out that the thermal condition of TP is only one of the most important factors to impact the ASM precipitation. While other factors (e.g., ENSO, NAO, aerosol) may affect the ASM precipitation (Yu and Zhou, 2004; Cheng *et al.*, 2005), there is no agreement on which factor plays a dominated role. It is worthy of further study to determine whether or not TP heat source depends on other factors. For example, in addition to vegetation and soil moisture, tropospheric temperature and snow cover are influenced also by ENSO (Yang, 1996; Miyakoda *et al.*, 2003; Shaman and Tziperman, 2005) and atmospheric teleconnection (Lu *et al.*, 2008), which will be our future research topics.

References

Chang C-P. 2004. *World Scientific Series on Meteorology of East Asia, Vol 2: East Asian Monsoon*, World Scientific: New Jersey, USA; 572.

Chen M, Shi W, Xie P, Silva VBS, Kousky VE, Higgins RW, Janowiak JE. 2008. Assessing objective techniques for gauge-based analyses of global daily precipitation. *Journal of Geophysical Research* **113**(D04): 110. DOI: 10.1029/2007JD009132.

Cheng Y, Lohmann U, Zhang J, Luo Y, Liu Z, Lesins G. 2005. Contribution of changes in sea surface temperature and aerosol loading to the decreasing precipitation trend in Southern China. *Journal of Climate* **18**: 1381–1390.

Chow KC, Chan JCL, Shi XL, Liu YM, Ding YH. 2008. Time-lagged effects of spring Tibetan Plateau soil moisture on the monsoon over China in early summer. *International Journal of Climatology* **28**: 55–67.

Ding YH. 1992. Summer monsoon rainfalls in China. *Journal of the Meteorological Society of Japan* **70**: 373–396.

Ding YH, Sun Y, Wang Z, Zhu Y, Song Y. 2009. Inter-decadal variation of the summer precipitation in China and its association with decreasing Asian summer monsoon, Part II: possible causes. *International Journal of Climatology* **29**: 1926–1944.

Duan AM, Wu G. 2008. Weakening trend in the atmospheric heat source over the Tibetan Plateau during recent decades. Part I: observations. *Journal of Climate* **21**: 3149–3164.

Hsu H-H, Liu X. 2003. Relationship between the Tibetan Plateau heating and East Asian summer monsoon rainfall. *Geophysical Research Letters* **30**: 2066. DOI: 10.1029/2003GL017909.

Kanamitsu M, Ebisuzaki W, Woollen J, Yang S-K, Hnilo JJ, Fiorino M, Potter GL. 2002. NCEP-DOE AMIP-II reanalysis (R-2). *Bulletin of the American Meteorological Society* **83**: 1631–1643.

Li C, Yanai M. 1996. The onset and interannual variability of the Asian summer monsoon in relation to land-sea thermal contrast. *Journal of Climate* **9**: 358–375.

Liu H-Q, Sun Z-B, Wang J, Min J-Z. 2004. A modeling study of the effects of anomalous snow cover over the Tibetan Plateau upon the South Asian summer monsoon. *Advances in Atmospheric Sciences* **21**: 964–975.

Lu J-M, Ju J-H, Kim S-J, Ren J-Z, Zhu Y-X. 2008. Arctic oscillation and the autumn/winter snow depth over the Tibetan Plateau. *Journal of Geophysical Research* **113**(D14): 117. DOI: 10.1029/2007J009567.

Miyakoda K, Kinter JL, Yang S. 2003. The role of ENSO in the south Asian monsoon and pre-monsoon signals over the Tibetan Plateau. *Journal of the Meteorological Society of Japan* **81**: 1015–1039.

Murakami T. 1988. Monsoon Meteorology. In *Oxford monographs on geology & geophysics no. 7*, Chang C-P, Krishnamurti T (eds). Oxford University Press: Oxford; 235–270.

Nan S, Zhao P, Yang S, Chen J. 2009. Springtime tropospheric temperature over the Tibetan Plateau and evolutions of the tropical Pacific SST. *Journal of Geophysical Research* **114**(D10): 104. DOI: 10.1029/2008JD011559.

Qian YF, Zheng YQ, Zhang Y, Miao MQ. 2003. Responses of China's summer monsoon climate to snow anomaly over the Tibetan Plateau. *International Journal of Climatology* **23**: 593–613.

Shaman J, Tziperman E. 2005. The effect of ENSO on Tibetan Plateau snow depth: a stationary wave teleconnection mechanism and implications for the south Asian monsoons. *Journal of Climate* **18**: 2067–2079.

Wang B, Bao Q, Hoskins B, Wu G, Liu Y. 2008. Tibetan Plateau warming and precipitation change in East Asia. *Geophysical Research Letters* **35**(L14): 702. DOI: 10.1029/2008GL034330.

Wang Y, Zhao P, Yu R, Rasul G. 2009. Inter-decadal variability of Tibetan spring vegetation and its associations with eastern China spring rainfall. *International Journal of Climatology* **30**: 856–865.

Wei L, Li DL. 2003. Evaluation of NCEP/DOE surface flux data over Qinghai-Tibet plateau. *Plateau Meteorology* **22**: 478–487. (in Chinese).

Wu T, Qian Z. 2003. The relation between the Tibetan winter snow and the Asian summer monsoon and rainfall: an observational investigation. *Journal of Climate* **16**: 2038–2051.

Yanai M, Wu G-X. 2006. Effects of the Tibetan Plateau, chapter 13. In *The Asian Monsoon*, Wang B (ed.) Springer: Berlin, Germany; 513–549.

Yang S. 1996. ENSO-snow-monsoon associations and seasonal-interannual predictions. *International Journal of Climatology* **16**: 125–134.

Yin D. 1986. 600 hPa circulation systems over the Qinghai-Xizang Plateau and south Asia in the summer, 1979, *Proceedings of the International Symposium on the Qinghai-Xizang Plateau and Mountain Meteorology, Beijing, China*, Science Press: 414–434.

Yu R, Zhou T. 2004. Impacts of winter-NAO on March cooling trends over subtropical Eurasia continent in the recent half century. *Geophysical Research Letters* **31**(12): L12204. DOI: 10.1029/2004GL019814.

Zhang YS, Li T, Wang B. 2004. Decadal change of the spring snow depth over the Tibetan Plateau: the associated circulation and influence on the East Asian summer monsoon. *Journal of Climate* **17**: 2780–2793.

Zhao TB, Fu CB. 2009. Applicability evaluation for several reanalysis datasets using the upper-air observations over China. *Chinese Journal of Atmospheric Sciences* **33**: 634–648 (in Chinese).

Zhao P, Zhou Z, Liu J. 2007. Variability of Tibetan spring snow and its associations with the hemispheric extratropical circulation and East Asian summer monsoon rainfall: an observational investigation. *Journal of Climate* **20**: 3942–3955.

Zhou T, Gong D, Li J, Li B. 2009. Detecting and understanding the multi-decadal variability of the East Asian Summer Monsoon: recent progress and state of affairs. *Meteorologische Zeitschrift* **18**: 455–467.

Zhou T, Zou L. 2010. Understanding the Predictability of East Asian Summer Monsoon from the Reproduction of Land-Sea Thermal Contrast Change in AMIP-type Simulation. *Journal of Climate* **23**: 6009–6026.